

Flame Extinction Limits in CH₂F₂/Air Mixtures

CAROLE WOMELDORF* and WILLIAM GROSSHANDLER

Building and Fire Research Laboratory, National Institute of Standards and Technology,
Gaithersburg, MD 20899, USA

To optimize the efficiency and safety of mixtures of nonozone-depleting refrigerant replacements, precise measurements of the lean flammability limits of pure refrigerants and the critical flammability ratio of their mixtures are crucial. Current test methods that model the accidental ignition of a volume of premixed fuel and air provide ambiguous results when measuring the limiting behavior of weakly flammable refrigerants. An alternative approach using the extrapolation of the global extinction stretch rates to zero as measured in a premixed counterflow burner has been tested. In this work the approach, accuracy, and precision of the technique as it applies to CH₂F₂ (difluoromethane, R-32) are presented. Comparisons are made to the behavior of CH₄ in the same burner and to published data on the lean limiting equivalence ratio, Φ_0 . The lean flammability limit of CH₂F₂ in dry air is found to be $\Phi_0 = 0.78 \pm 0.04$. Concurrent computational modeling of the combustion of a one-dimensional, unstrained flame of CH₂F₂ in air, individually and in mixtures with CH₄, has been performed. Initial estimates of the laminar flame speed for CH₂F₂/air mixtures from stoichiometric to lean are reported and interpreted in light of the experimental results. © 1999 by The Combustion Institute

BACKGROUND

The phase-out of chlorofluorocarbons (CFCs) and some hydrochlorofluorocarbons (HCFCs) due to their ozone depletion potential has forced the air-conditioning and refrigeration industry to search for alternative refrigerants. In the 1950s, refrigerants were selected because they possessed the optimum qualities: high efficiency and nonflammability. With ozone depletion potential and global warming as new considerations, refrigerants that were once considered less than ideal are being reexamined. Potential replacements must meet current residential building codes in the United States that prohibit the use of flammable refrigerants in most applications. Mixtures of the flammable refrigerant difluoromethane (CH₂F₂) with other nonflammable refrigerants are strong candidates to satisfy requirements of nonflammability, efficiency, and the environmental criteria. Because a precise and accurate measurement of the flammability differences among weakly flammable refrigerant alternatives is of great importance, a detailed examination of the extinction characteristics of CH₂F₂ has been conducted.

Difluoromethane, commonly referred to as R-32, is a nontoxic gas with a vapor pressure of 1.59 MPa at room temperature (25°C) and a

molecular weight of 52 g/mol. Its normal boiling point is -52°C, and it has a critical temperature and pressure of 78.4°C and 5.83 MPa, respectively. The enthalpy of formation of CH₂F₂ is -8.7 MJ/kg and the heat of combustion is -3.5 MJ/kg, as compared to -4.6 MJ/kg and -50 MJ/kg, respectively, for methane (CH₄). Figure 1 is a plot of the product mole fractions and temperatures of adiabatic equilibrium mixtures of CH₂F₂ and air at atmospheric pressure as a function of the fuel/air equivalence ratio, Φ [1]. During combustion, fluorine acts as an oxidizer, converting most of the H-atoms to HF. Only one molecule of O₂, with the associated 3.76 molecules of N₂ in air, is required to oxidize the remaining single carbon atom to CO₂. Because of the relatively small amount of inert nitrogen, the adiabatic equilibrium temperature of a stoichiometric mixture of CH₂F₂ in air is almost as high as that of CH₄. The peak temperature is 1940°C, occurring on the rich side of stoichiometric. Hydrogen fluoride makes up about 30% of the product species. The CO mole fractions are similar to those found in CH₄/air mixtures, but the equilibrium OH mole fractions are more than an order of magnitude lower. The mole fraction of equilibrium H₂ does not exceed 5×10^{-6} in the CH₂F₂ system, as compared to greater than 0.02 mole fraction in CH₄/air combustion.

The current American Society for Testing and Materials (ASTM) method the refrigera-

*Corresponding author. E-mail: cwomeldorf@nist.gov

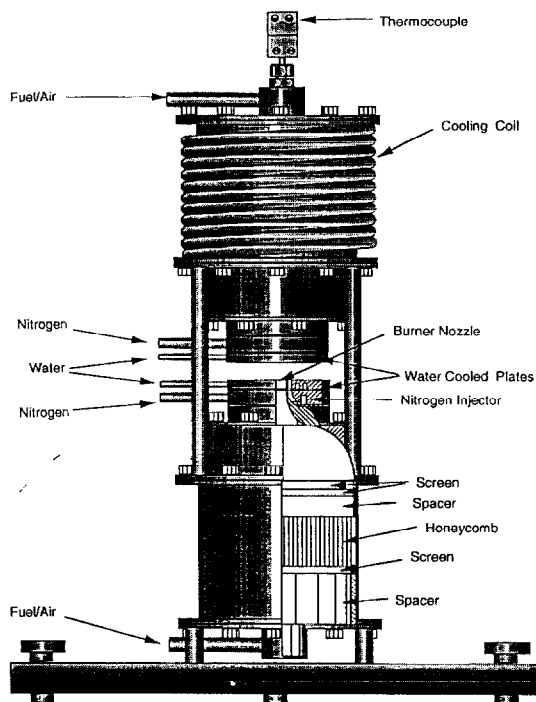


Fig. 2. Counterflow burner assembly shown with a partial cutaway of the lower nozzle section.

ment, and a flow control system. A comprehensive description of the test facility is contained in an earlier report [7]. The primary component is the burner, shown in Fig. 2, made of 304 stainless steel to resist the corrosive effects of the hazardous combustion byproduct, hydrofluoric acid (HF). The critical dimensions of the burner are the nozzle separation and the nozzle diameter, both of which are fixed at $12.0 \text{ mm} \pm 0.1 \text{ mm}$. Inside the cylindrical section above the nozzle, the incoming gases are conditioned with a honeycomb section and fine mesh screens. The converging nozzle is designed from two matched cubic contours following the criteria of Morel [8], with an area contraction ratio of 44 to 1. Nitrogen flows in a thin concentric annulus. The burner surfaces directly exposed to the flames are water cooled to minimize preheating of the reactants. A copper tube flows water around the upper chamber to reduce heating by exhaust gases. A thermocouple along the centerline of the upper section, placed just above the contraction of the nozzle, monitors the incoming gas temperature.

The CH_2F_2 has a minimum purity of 0.998

mole fraction and is stored as a liquid at room temperature and 1.6 MPa. The supply bottle is connected to a lower pressure expansion tank to provide a steady flow of gas. In the CH_4 , air and ethane are the largest contaminants, but the minimum purity is 0.9995 mole fraction. The air is certified to have a mole fraction of O_2 equal to 0.2110 ± 0.0002 , with water and hydrocarbon levels below 10^{-6} . The remaining components (N_2 , Ar, and CO_2) are as taken from the atmosphere.

The gas flows are controlled with individual high accuracy mass flow controllers. Gas pressures into the controllers are regulated at $138 \text{ kPa} \pm 3 \text{ kPa}$ to standardize initial flow conditions. The air and selected fuel are mixed at a tee just beyond the flow controls. The mixture is split between the upper and lower sections near the burner. To maximize the resolution of the mass flow controller signal, the resolution of the gas controller was increased from 0.1% to 0.01% of the full scale for each controller. All flow controllers are calibrated to $\pm 2\%$ of value with the gas used during testing. The calibration reference is a digital bubble flow meter. This flow meter was tested using the National Institute of Standards and Technology (NIST) standard piston prover and has been shown [9] to be accurate to within $\pm 1\%$ over its entire range, 0.1 L/m to 25 L/min. Local barometric pressure was acquired by the computer from a precision barometer with an accuracy of 0.015% of reading.

The flame is ignited at an equivalence ratio richer than the expected lean flammability limit for the given stretch rate, but lean enough to avoid flashback into the burner. Once ignited, the twin flame is visible on a video monitor. Depending on the conditions, the luminescent region is 10 mm to 20 mm in diameter and the dark zone gap between the flames is about 4 mm or less. The N_2 shroud is initiated once the flame is stable, lifting and truncating the outer edge of the flame. During an experiment, the equivalence ratio is reduced in small increments while the stretch rate is held constant. At each step-change the flames move closer together and then restabilize, until the merged flames extinguish. A typical extinction point takes less than 7 minutes to determine.

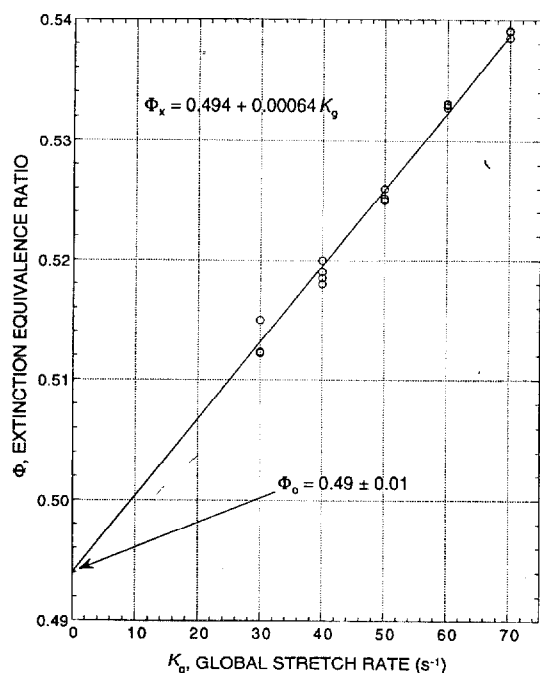


Fig. 3. Lean extinction points for different global stretch rates for CH_4 in dry air.

EXPERIMENTAL RESULTS

CH_4/Air

The motivation behind the methane testing was to ensure that the limiting lean equivalence ratio, Φ_0 , measured with the NIST counterflow burner agreed with published results using other techniques. Figure 3 is a plot of multiple CH_4 extinction points taken with global stretch rates between 30 s^{-1} and 70 s^{-1} inclusive. Together they define the low stretch, lean perimeter of the flammability of CH_4 in dry air. The line

described by $\Phi_x = 0.494 + 0.00064 \cdot K_g$ was derived from a linear fit, where Φ_x is the equivalence ratio at extinction and K_g is the corresponding global stretch rate. Assuming the linear extrapolation technique holds, the intercept corresponds to the lean flammability limit of $\text{CH}_4/\text{dry air}$ mixtures at about 99 kPa and 27°C . The standard deviation of the fit is 0.2% of the intercept value for a 95% confidence interval. This low statistical uncertainty indicates the high repeatability of the experiments and suggests that the fit is close to linear over the range of 30 s^{-1} to 70 s^{-1} under these normal gravity conditions. The total uncertainty in Φ_0 is dependent also upon the uncertainty in the flow calibrations. Accounting for these as well leads to a lean flammability limit of $\Phi_0 = 0.49 \pm 0.01$ with a 95% confidence interval.

The lean limit equivalence ratio for CH_4 measured in this burner can be compared with the published values listed in Table 1. Our value falls comfortably in the middle of the range. The lowest value in the table, 0.4, represents an extreme based on a test which measures the extinction concentration at the tip of a flame while the mixture is encircled by another flame. In describing their technique, Sorenson et al. [14] state that their method is "... not intended to supplant standard flammability techniques that measure the flame's ability to propagate..." Hence, a value of 0.4 may not be a valid comparison point. The highest value in the table, 0.51, was determined using the 5-L volume ASTM apparatus [10].

That the current value for the lean flammability limit falls within the range determined by others may be fortuitous considering that two

TABLE 1

Lean Flammability Limits of CH_4/Air Using Different Experimental Methods

Author(s)	Method	Conditions	CH_4/Air Lean Limit, Φ_0
Richard and Shankland [10]	ASTM E 681	5 liter, match ignition	0.51
Zabetakis [11]	Propagating flame tube	Extinction	0.50
This work	Counterflow, twin flame	Linear extrapolation	0.49 ± 0.01
Richard and Shankland [10]	ASTM E 681	5 liter, match ignition	0.48
Ishizuka and Law [12]	Counterflow, twin flame	Linear extrapolation	0.48
Yamaoka and Tsuji [13]	Tsuji burner	Flame location	0.47
Maruta et al. [4]	Counterflow, twin flame, $\mu\text{-g}$	Turning point	0.47
Sorenson et al. [14]	Coaxial (tent) flame	Flame angle	0.40

major assumptions were made in reducing the data: (1) the stretch rate vs equivalence ratio curve is linear in the zero-stretch limit, and (2) the global stretch rate characterizes the local stretch rate. As mentioned earlier, recent experimental [4] and theoretical studies [5] have demonstrated that in μ -gravity the extinction equivalence ratio does not in fact approach the zero-stretch condition in a linear fashion. However, the purpose of our approach is the design of a flammability limit test procedure for the determination of the lean limit under typical laboratory conditions, and the value of $\Phi_0 = 0.49$ is within 6% of the lean limit determined experimentally in μ -gravity by Maruta et al. [4].

Support for assumption (2) is provided by Kobayashi and Kitano [15], who plotted local stretch rates measured with a laser Doppler velocimeter against the global stretch rate for their twin flame, counterflow burner operating on methane/air mixtures. While the relation between global and local stretch rate was found to vary with the burner separation (12 mm or 18 mm), in both cases the curve was linear under lower stretch conditions and passed through the origin. It is not necessary for the global and local flame stretch rates to be equal to each other, just that they remain proportional for a fixed geometry.

$\text{CH}_2\text{F}_2/\text{Air}$

The $\text{CH}_2\text{F}_2/\text{air}$ flame was operated in a manner similar to the CH_4/air flame. Because the primary product of CH_2F_2 combustion is HF, all experiments were performed inside a chemical hood. This refrigerant flame is much more difficult to ignite than the CH_4 flame. In overall appearance, the CH_2F_2 flame is whitish blue, and is somewhat thicker and brighter than the CH_4 flame, even when near the extinction limit.

Figure 4 is a plot of the equivalence ratio at extinction over a range of global stretch rates for CH_2F_2 in dry air at 100 kPa and 26°C. A linear extrapolation to zero stretch produces an intercept value of 0.78 with a 95% confidence interval of ± 0.04 . A significant difference between a hydrofluorocarbon and a hydrocarbon flame is evident when comparing Figs. 3 and 4. At the highest global stretch rate tested, 70 s^{-1} , the extinction equivalence ratio for CH_2F_2

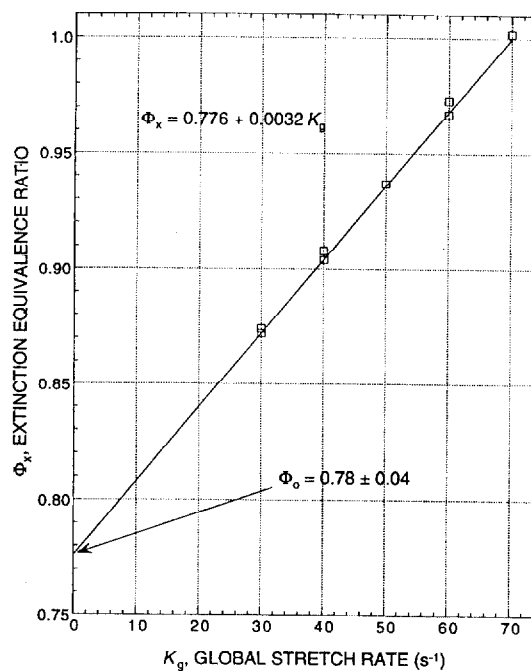


Fig. 4. Lean extinction points for different global stretch rates for CH_2F_2 in dry air.

equals 1.0, whereas for CH_4 it is only 0.54. The slope of the Φ_0 vs K_g line is more than 50% steeper for the CH_2F_2 flame. It is evident from these experimental results that CH_2F_2 is a much weaker fuel than CH_4 for lean to stoichiometric combustion.

Table 2 shows a comparison of the lean flammability limits measured in $\text{CH}_2\text{F}_2/\text{air}$ mixtures from different authors. The current results fall in the middle and agree with values published by Dekleva et al. [16] using both a 5-L and 12-L ASTM E 681 device. Overall, the range of values is much wider than those published for CH_4 . This may be attributed to the effect of uncertain stretch rates in the different techniques and the sensitivity of a weakly flammable fuel to heat losses to the vessel or heat additions from an ignition source. The relatively steep slope shown in Fig. 4 supports the argument that a small change in stretch can have a large impact on the extinction value.

FLAME STRUCTURE CALCULATIONS

The experimental measurements indicate that the $\text{CH}_2\text{F}_2/\text{air}$ flame is much less robust when

TABLE 2

Lean Flammability Limits of CH₂F₂/Air Using Different Experimental Methods

Author(s)	Method	Conditions	CH ₂ F ₂ /air Lean Limit, Φ_0
Dekleva et al. [16]	5-cm tube (ICI)	Hot wire	1.11
Richard and Shankland [10]	4-liter tube	Match	0.84
Dekleva et al. [16]	ASTM E 681, 5 liter	Hot wire	0.81
Grob [17]	ASTM E 681, 12 liter	Hot wire	0.81
Richard and Shankland [10]	ASTM E 681, 5 liter	Hot wire	0.79
This work	Counterflow, twin flame	Linear extrapolation	0.78 ± 0.04
Dekleva et al. [16]	ASTM E 681, 5 liter	Hot wire	0.77
Dekleva et al. [16]	ASTM E 681, 12 liter	Match	0.77
Dekleva et al. [16]	Autoclave, 8 liter	Hot wire	0.75
Richard and Shankland [10]	ASTM E 681, 5 liter	Spark	0.74
Ohnishi [18]	ASTM E 681, 5 liter	Paper match	0.71
Richard and Shankland [10]	ASTM E 681, 5 liter	Match	0.69

compared to the CH₄/air flame at the same equivalence ratio. The blue chemiluminescent region is also noticeably thicker in the refrigerant flame. Computational representations of the two flames can be used to help explain these experimental observations.

The extinction of symmetric counterflow hydrocarbon/air flames has been numerically modeled with some success by a number of researchers [19, 20]. The addition of fluorine to the hydrocarbon kinetics scheme greatly expands the number of molecular species that need to be tracked in the calculations. The computational penalty associated with including a complete chemical kinetics package such as the one developed by Burgess et al. [21], renders a two-dimensional, buoyant, counterflow model impractical, and may be unnecessary to explain the qualitative differences between methane and difluoromethane flames.

As a tractable alternative, the flames were assumed to be one-dimensional, freely propagating, and adiabatic. The structure of such a flame can be calculated in a straightforward manner using the PREMIX code [22] developed by Sandia National Laboratories with the chemical kinetics package CHEMKIN [23]. The methane/air chemistry was based upon the Gas Research Institute (GRI) mechanism [24], while the F/C/H/O mechanism developed by Burgess et al. [21] was used to model the detailed fluorine chemistry with reactions up to C₂. A total of 780 chemical reactions were assumed to take place among 81 species.

The PREMIX flame code has a number of options which control the calculation procedure and can impact the predicted species mole fractions, temperature profile, and flame speed. In the current study the secondary effect of the temperature gradient on mass diffusion (Soret effect) was included. Up-wind differencing was used for the convective term, and the flame was assumed to be anchored at the location where the temperature reached 127°C. The parameters GRAD and CURV control the development of the grid spacing, with small values of each restraining the maximum first and second derivatives in the species profiles that will be tolerated. The former was set at 0.1 and the latter at 0.3. The absolute and relative tolerances placed on convergence of the Newton iteration were 1.0×10^{-9} and 1.0×10^{-4} , respectively.

The required number of grid points across the flame in a converged solution ranged between 126 for a stoichiometric CH₄/air flame to 238 for a CH₂F₂/air flame approaching its lean flammability limit. The computational domain extended from -50 mm to +1000 mm. The numerical program as received from Sandia National Laboratory was designed to run on a work-station, but the code was modified for the current effort to be compatible with the NIST Convex C3820 vector machine. Depending upon the initial conditions in the problem and the accuracy of the first guess for the temperature profile, it took from 1000 s to 40,000 s of CPU time to reach a converged solution.

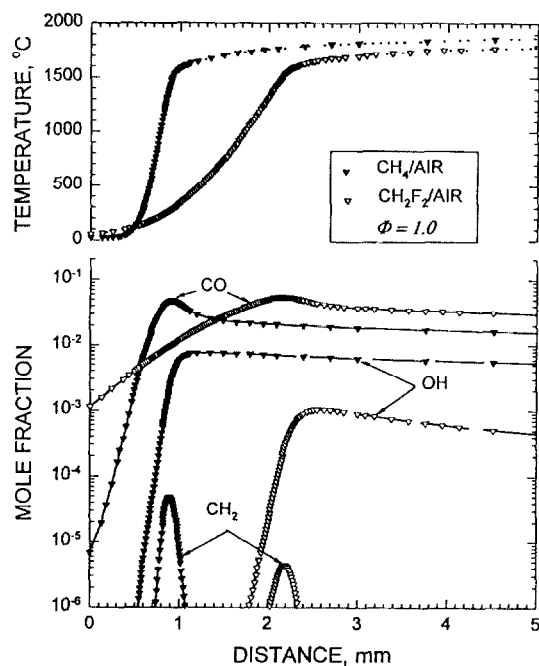
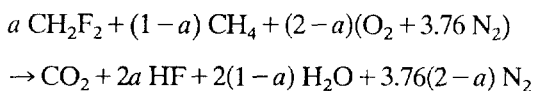


Fig. 5. Computed temperature and species profiles through one-dimensional methane/air and difluoromethane/air flames at atmospheric pressure.

Stoichiometric CH₄/CH₂F₂/Air Mixtures

The complete combustion of a mixture of CH₄ and CH₂F₂ at an overall equivalence ratio of unity is given by the following expression:



where a is the mole fraction of CH₂F₂ in the binary fuel. Computations were performed, first, in the limiting cases of $a = 1$ and $a = 0$ to compare the structure of a pure CH₂F₂/air flame to that of a CH₄/air flame.

The upper graph in Fig. 5 is a plot of the temperature in the two flames. The initial temperature at the left is 25°C. In the CH₄ flame, the temperature rises steeply within the first millimeter and reaches 1960°C by the end of the computational domain. The temperature in the CH₂F₂ flame builds up more slowly but eventually reaches almost the same value (1930°C). By transforming the distance scale to a time scale, the temperature-time gradient can be used to accentuate the difference in temperature buildup within each of the two stoichiometric

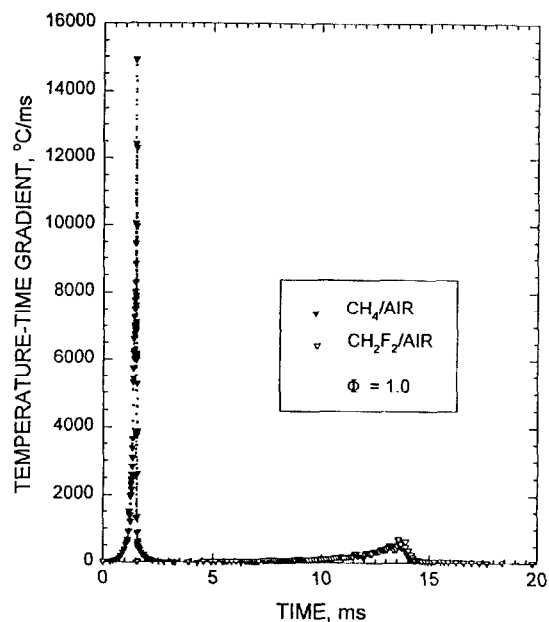


Fig. 6. Computed rate-of-temperature increase across one-dimensional flame, comparing difluoromethane/air and methane/air mixtures.

flames, as seen in Fig. 6. The magnitude of the methane/air peak is 25-fold greater than the magnitude of the difluoromethane/air peak, and the methane peak occurs almost an order of magnitude earlier in time.

The lower portion of the graph in Fig. 5 compares the mole fractions of CO, OH, and CH₂ (ground-state) in the CH₄ and CH₂F₂ flames. The carbon monoxide begins to form earlier in the CH₂F₂ flame, but the rate of formation of CO in the CH₄ flame accelerates and reaches its maximum mole fraction sooner, followed by a decay to the final equilibrium value. The peak CO mole fraction is about the same in both flames. The OH mole fraction is indicative of the size of the chain-propagating radical pool, and is shown to peak in the CH₂F₂ flame beyond the CO. The level of OH is about an order of magnitude smaller than the OH in the CH₄ flame. The ground-state triplet methylene (CH₂) behaves in a way representative of other small hydrocarbon radicals (e.g., CH₃, CH). It reaches a peak at a location close to that of the CO, and then practically disappears shortly beyond the OH maximum for both fuels. The mole fraction of CH₂ in the CH₂F₂ flame is over 10 times lower than in the methane flame.

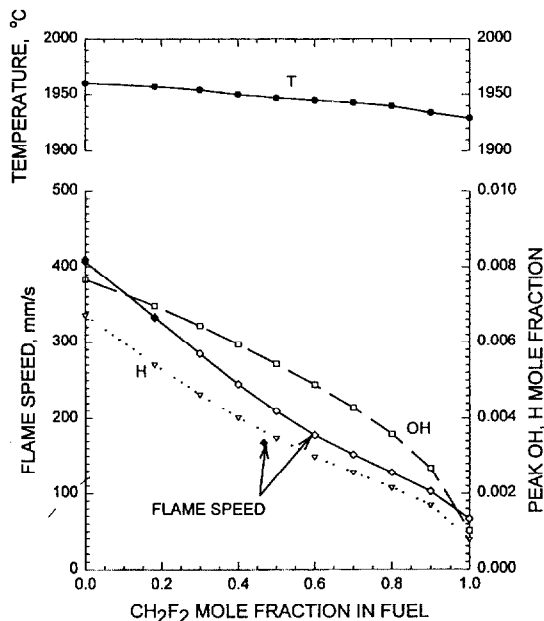


Fig. 7. Computed effect of replacing CH_4 with CH_2F_2 on stoichiometric flame speed (open diamonds), equilibrium temperature (filled circles), and peak mole fractions of H (open triangles) and OH radicals (open squares). Experimental flame speeds of Linteris and Truett [6] are shown as filled diamonds.

When the CH_2F_2 and CH_4 are combined into a single flame, the calculated normal flame speed, v_0 , for a stoichiometric mixture decreases from 407 mm/s to 67 mm/s as a , the mole fraction of refrigerant, is increased from 0 to 1.0. The calculated flame speed for pure CH_4/air is in agreement with measurements and the rough calculations by Linteris and Truett [6], although they and others (e.g., [25]) have stated that increasing the number of grid points indefinitely reduces the calculated flame speed to less than 390 mm/s. The numerical uncertainty in the current calculations, in general, is estimated to be ± 20 mm/s based upon repeated calculations using different initial temperature profiles and grid control parameters. The calculated flame speeds are shown in Fig. 7, along with the final flame temperatures and maximum OH and H mole fractions. The flame temperature varies only slightly with the fraction of CH_2F_2 , whereas the OH and H drop monotonically to less than 15% of their initial value as a is increased from 0 to 1.

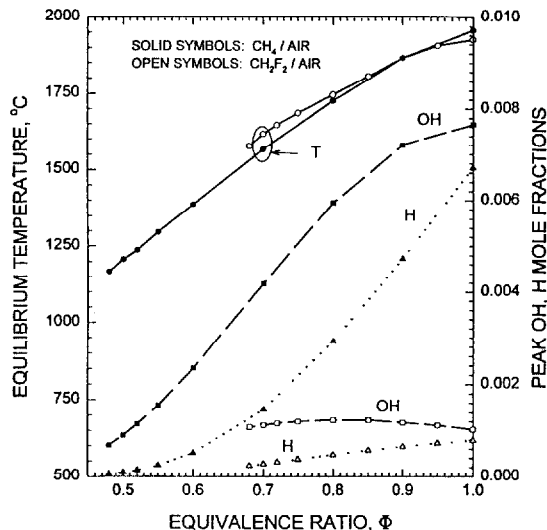


Fig. 8. Computed equilibrium temperature and peak OH and H radical mole fractions as a function of equivalence ratio, comparing methane/air to difluoromethane/air flames.

Lean $\text{CH}_2\text{F}_2/\text{Air}$ Mixtures

The impact of equivalence ratio, Φ , on the structure of the pure $\text{CH}_2\text{F}_2/\text{air}$ flame also has been examined numerically, and compared to the impact of Φ on the CH_4/air flame. Figure 8 is a plot of the final temperatures and peak OH and H mole fractions as a function of equivalence ratio. As one would expect, the temperature of the refrigerant flame decreases continuously with decreasing Φ . It is noteworthy, however, that the final temperature in the CH_2F_2 flame exceeds that of the methane flame when the equivalence ratio is leaner than 0.90. Of great significance is the difference in behavior of the peak OH mole fraction for the two fuels. For the $\text{CH}_2\text{F}_2/\text{air}$ flame, not only is the level of the OH much less, but also the shape of the curve is qualitatively different. The calculated OH mole fraction in the methane/air flame drops by a factor of 10 as Φ changes from 1.0 to 0.5, and H-atom by a factor of 100. In the $\text{CH}_2\text{F}_2/\text{air}$ flame the OH mole fraction actually increases slightly as the flame moves from stoichiometric to $\Phi = 0.8$, but remains close to 0.001 over the entire range of equivalence ratios examined. The H-atom mole fraction decreases monotonically with Φ , but not as steeply as calculated for the CH_4/air flame.

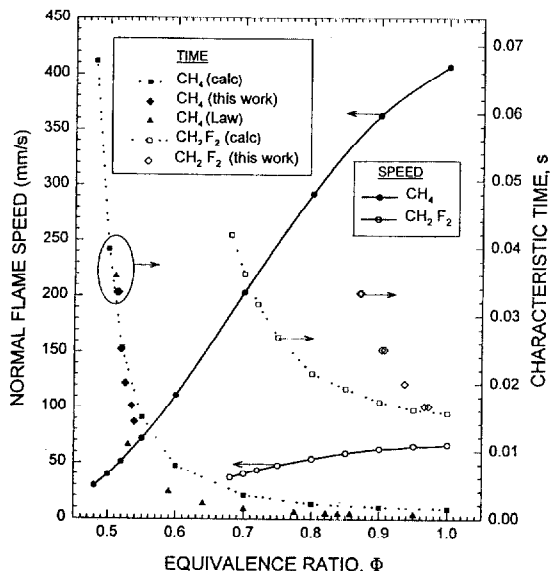


Fig. 9. Effect of equivalence ratio on computed flame speed and characteristic time for chemical reaction, compared to estimated residence time in experimental flames at extinction.

Figure 9 compares the propagation speeds for the two flames at different values of Φ . The normal flame speed drops slowly with decreasing Φ in the $\text{CH}_2\text{F}_2/\text{air}$ flame, eventually attaining a value of 36.7 mm/s for $\Phi = 0.68$. The numerical model computes a value of 29 mm/s for an unstretched, adiabatic methane/air flame at an equivalence ratio of 0.48.

DISCUSSION OF RESULTS

Very few experiments have been reported in the literature on $\text{CH}_2\text{F}_2/\text{air}$ flames. Aside from the flammability limit measurements referenced in Table 2, the work by Linteris and Truett [6] is the sole experimental study in which the speed of a $\text{CH}_2\text{F}_2/\text{CH}_4/\text{air}$ flame has been explicitly determined. They used a premixed, laminar coflow burner in which increasing amounts of CH_2F_2 were added to an initially lean, stoichiometric or rich methane/air flame. The flame speed was determined from Schlieren photographs of the flame cone angle. The solid diamonds plotted in Fig. 7 are their data. The measured flame speeds at $a = 0$ and $a = 0.18$ are within the uncertainty of those predicted by the PREMIX model. For the highest mole

fraction of CH_2F_2 studied in the experimental flame ($a = 0.46$), the overall equivalence ratio was about 1.20 (even though Φ based upon the methane/air ratio was 0.9). The difference in equivalence ratios between their measurement and the PREMIX prediction (in which $\Phi = 1.0$) may account for the 45 mm/s discrepancy in flame speed. This was not confirmed with PREMIX because the fluorine mechanism is uncertain in rich mixtures.

The counterflow burner results presented earlier in this paper cannot be predicted directly from the PREMIX/CHEMKIN calculations since flame stretch, heat loss, and buoyancy have been excluded. Because these natural quenching processes are absent, the numerical code predicts a nonzero flame propagation rate for mixtures leaner than the experimental flammability limit. Westbrook [26] suggested that mixtures with one-dimensional, adiabatic flame speeds predicted to be less than 50 mm/s are beyond the flammability limit from a practical standpoint. Bui-Pham et al. [27] considered a similar criterion for identifying the rich flammability limit of a methanol/ CO/air mixture, and found it to correspond to the condition where the rate of the primary chain branching reaction ($\text{H} + \text{O}_2 \rightarrow \text{OH} + \text{H}$) is equal to the rate of the primary chain terminating reaction ($\text{H} + \text{HO}_2 \rightarrow \text{H}_2 + \text{O}_2$), as suggested originally by Law and Egolfopoulos [28]. Using 50 mm/s as a qualitative measure of the flammability boundary, then, the current study predicts a practical lean flammability limit of 0.52 for CH_4/air and 0.77 for $\text{CH}_2\text{F}_2/\text{air}$.

Chung et al. [29] demonstrated that extinction is likely when the fluid mechanical residence time in the flame is less than the characteristic chemical reaction time. A characteristic fluid residence time, τ_f , can be estimated from the conditions in the experimental burner and compared to the characteristic time for chemical reaction, τ_c , as estimated from the numerical simulation. The characteristic fluid residence time scales with the distance between the burner outlet and the stagnation plane, divided by the outlet velocity (i.e., the inverse of the global stretch rate, $1/K_g$). The residence times at the extinction limit as measured in the current study are plotted in Fig. 9. The open diamond symbols correspond to the $\text{CH}_2\text{F}_2/\text{air}$

flame and the filled diamonds refer to the CH₄/air flame. Also plotted in Fig. 9 (solid triangles) is the inverse of the stretch rate near extinction which was determined by Law et al. in their counterflow, premixed methane/air burner, using the slope of the local velocity on the center line in the preheat zone [3]. The two CH₄ flame data sets are in reasonable agreement, suggesting that the *global* stretch rate at extinction may reasonably approximate the *local* strain rate at extinction for the lean conditions examined in the current study, a conclusion also reached by Maruta et al. [4] based upon the work of Kobayashi and Kitano [15].

The dotted lines shown in Fig. 9 are drawn through the characteristic reaction times, τ_c , determined from the PREMIX/CHEMKIN results (symbolized by the open and filled squares for CH₂F₂ and CH₄ flames, respectively). The reaction time is approximated by the transit time between the location of the flame anchoring temperature, 127°C (as suggested in [22]), and the position of the peak H mole fraction. The peak in H was selected as a marker for reaction time because of the importance of H-atom to flame propagation, and because the peak was found at a location close to the maximum levels of OH, a radical critical to the burnout of CO.

By comparing the numerically calculated τ_c to the experimentally determined τ_f , one can see that extinction in the actual stretched CH₄/air flame is predicted reasonably well by the PREMIX model when the two characteristic times are about equal to each other. The same cannot be said of the CH₂F₂/air flame. The numerical calculations suggest that, for all equivalence ratios leaner than 0.9, the flame should be more robust than the experimental data indicate. This discrepancy may be explained in four possible ways.

A first possibility is that the radiative and conductive heat losses, which are not included in model, are more significant (and therefore more detrimental) to the refrigerant flame than to the hydrocarbon flame. While radiation heat loss has been included by others in PREMIX models of hydrocarbon flames [30], an estimate of the relative importance of the radiation in the two flames studied here can be made by following the approach of Hertzberg [31]. The heat

loss due to radiation leads to a limiting flame speed of $\sigma k_p l_r T_f^3 / c_p \rho$, where σ is the Stefan-Boltzmann constant, k_p is the gray gas absorption coefficient, l_r is the radiation length scale, c_p is the specific heat of the flame, and ρ is the gas density. This limiting flame speed can be compared for each of the fuels at $K_g = 40 \text{ s}^{-1}$, corresponding to an extinction equivalence ratio of 0.90 for the CH₂F₂/air flame, and $\Phi = 0.52$ for methane. At these conditions, the calculated flame thicknesses are approximately the same, but the flame temperatures vary significantly: 2140 K for CH₂F₂/air and 1510 K for CH₄/air. Although there is some difference in k_p between the two fuels, it about cancels with the change in density due to temperature. As a result, the radiation flame speeds scale with T_f^3 , whence the effect of radiant heat loss is almost three times greater in the refrigerant flame than in the methane flame. The higher temperatures in the CH₂F₂/air flame also lead to greater heat loss to the cooled burner due to conduction, which scales with $\lambda \Delta T / l_c$ and can be significant due to the low gas velocities. The conduction length scale l_c is the same in each flame, but the product of the thermal conductivity, λ , and the temperature difference between the flame and the burner, ΔT , is just nearly twice as high in the refrigerant flame. The impact of heat loss on extinction prediction is, thus, more significant in the CH₂F₂/air flame, and adiabatic calculations of flame speed near the lean limit are more likely to overpredict experimental flame speeds (or underpredict flame residence time) when difluoromethane is the fuel.

A second explanation is that the inverse of the global stretch rate is not a good indicator of the fluid residence time in a CH₂F₂/air flame. Throughout this paper, the slope of the lines in Figs. 3 and 4 have not been suggested to precisely represent the true flame speed gradient, only that the intercepts with the zero stretch condition represent an accurate way to measure a lean flammability limit. This is supported by comparison to other results (see Tables 1 and 2, and ref. 15). Local velocity and temperature measurements are necessary to more accurately determine the fluid residence time.

An inappropriate choice from the chemical reaction time is a third possibility for the discrepancy in Fig. 9. The CO burnout region for

the CH_2F_2 /air flame is extended, compared to the methane flame at the same Φ , because the OH concentration is calculated to be much lower. However, at their respective lean limits the OH levels are similar in the two flames, suggesting that the rationale used to define τ_c is reasonable.

A final consideration is that the chemical kinetics mechanism is incomplete or contains incorrect rate coefficients for the fluorine-containing reactions. Linteris and Truett [6] found the same mechanism adequate to predict the flame speeds in their premixed CH_2F_2 -inhibited methane/air burner, but did not attempt to model the system with a fluorine/hydrogen ratio greater than 1:3. Considering the paucity of flame data under high fluorine loads like those modeled here, a large measure of uncertainty remains in the chemical kinetics scheme.

CONCLUSIONS

In this paper we have demonstrated that the counterflow burner is well suited for studying the structure of a pure CH_2F_2 /air flame. The flame is stable enough to investigate the relationship between equivalence ratio and the stretch rates necessary to extinguish the flame. A plot of the extinction equivalence ratio versus the global stretch rate shows the behavior to be linear down to flow rates where buoyancy begins to distort the flame (30 s^{-1}). At room temperature and pressure, extrapolation to the zero-stretch condition leads to a lean limit equivalence ratio for CH_2F_2 /dry air mixtures of 0.78 with a 95% confidence interval of ± 0.04 . This compares favorably to a range 0.69 to 0.81 as measured in the ASTM constant volume apparatus, and a value of 0.77 based upon a predicted one-dimensional, adiabatic flame speed of 50 mm/s.

Numerical simulations of one-dimensional, adiabatic methane and difluoromethane flames reveal striking differences in the two fuels. The mole fractions of radicals such as OH, H, and CH_2 are about an order of magnitude less in stoichiometric CH_2F_2 /air mixture than in CH_4 /air mixtures. While equilibrium flame temperatures are about the same in both, the peak time-rate-of-increase in temperature is 25 times

greater in the methane flame. The flame in the stoichiometric CH_2F_2 /air mixture is predicted to propagate at a speed only 16% of that for CH_4 /air mixtures. It is suggested that the higher temperatures in the difluoromethane flame near the lean limit contribute to the extinction loss mechanisms more so than in the methane flame.

It is concluded that the twin-flame, counterflow burner may be used to measure the lean flammability limit of a hydrofluorocarbon/air mixture at least as flammable as CH_2F_2 . Velocity measurements in the flame are required to determine more precisely the relation between local and global stretch rates. Even so, extrapolation to zero global stretch in the counterflow burner provides an attractive alternative to the ASTM E 681 apparatus for measuring the flammability limits of refrigerants.

This research was supported, in part, by the U.S. Department of Energy (Office of Building Technology) Grant DE-FG02-91CE23810: Materials Compatibility and Lubricants Research on CFC-Refrigerant Substitutes. Program management by Mr. Steven Szymurski of the Air-conditioning and Refrigeration Technology Institute is gratefully acknowledged. The authors would also like to thank Mrs. Michelle King Donnelly, Mr. Jaeson Howze, and Mr. William Rinkinen for their contributions.

REFERENCES

1. Gordon, S., and McBride, B. (1994). *Computer Program for Calculation of Complex Chemical Equilibrium Compositions and Application*. NASA Ref. Pub. 1311, NASA Scientific and Technical Information Program.
2. ASTM E 681-1994, "Standard Test Method for Concentration Limits of Flammability of Chemicals," American Society for Testing and Materials, Philadelphia, PA.
3. Law, C. K., Zhu, D. L., and Yu, G., *Twenty-First Symposium (International) on Combustion*, The Combustion Institute, 1986, p. 1419.
4. Maruta, K., Yoshida, M., Ju, Y., and Niioka, T., *Twenty-Sixth Symposium (International) on Combustion*, The Combustion Institute, 1996, pp. 1283-1289.
5. Sung, C. J., and Law, C. K., *Twenty-Sixth Symposium (International) on Combustion*, The Combustion Institute, 1996, pp. 865-973.
6. Linteris, G. T., and Truett, L., *Combust. Flame* 105:15 (1996).
7. Womeldorf, C. A., and Grosshandler, W. L. (1996) *Lean Flammability Limit as a Fundamental Refrigerant*

- Property, Phase II*: Interim Technical Report, DOE/CE/23810-68. The Air-conditioning and Refrigeration Technology Institute, ARTI MCLR Project No. DE-FG02-91CE23810.
8. Morel, T., *J. Fluids Eng.* 97(2):225 June (1975).
 9. Pitts, W. M., Mulholland, G. W., Breuel, B. D., Johnsson, E. L., Chung, S., and Harris, R. H., in *Fire Suppression System Performance of Alternative Agents in Aircraft Engine and Dry Bay Laboratory Simulations* (R. G. Gann, Ed.), NIST SP 890: Vol. II, Gaithersburg, MD, 1995, p. 348.
 10. Richard, R. G., and Shankland, I. R., *ASHRAE J.* 34(4):20 (1992).
 11. Zabetakis, M. G. (1965). *Flammability Characteristics of Combustible Gases and Vapors*. Bulletin 627, Bureau of Mines, National Technical Information Service, Springfield, VA.
 12. Ishizuka, S., and Law, C. K., *Nineteenth Symposium (International) on Combustion: The Combustion Institute*, 1982, p. 327.
 13. Yamaoka, I., and Tsuji, H., *Seventeenth Symposium (International) on Combustion: The Combustion Institute*, 1979, p. 843.
 14. Sorenson, S. C., Savage, L. D., and Strelow, R. A., *Combust. Flame* 24:347 (1975).
 15. Kobayashi, H., and Kitano, M., *Combust. Sci Technol.* 75:227 (1991).
 16. Dekleva, T. W., Lindley, A. A., and Powell, P., *ASHRAE J.* 35:40 (1993).
 17. Grob, D., *Proceedings of the Symposium to Evaluate R-32 and R-32 Mixtures in Refrigeration Applications*, Environmental Protection Agency, Washington, DC, March 19–20, 1991.
 18. Ohnishi, H., *Proceedings of the ASHRAE/NIST Refrigerants Conference: R-22/R-502 Alternatives*, Gaithersburg, MD, Aug. 19–20, 1993.
 19. Tanoff, M. A., Smooke, M. D., Osborne, R. J., Brown, T. M., and Pitz, R. W., *Twenty-Sixth Symposium (International) on Combustion*, The Combustion Institute, 1996, pp. 1121–1128.
 20. Egolfopoulos, F. N., Zhu, D. L., and Law, C. K., *Twenty-Third Symposium (International) on Combustion*, The Combustion Institute, 1990, pp. 471–478.
 21. Burgess, D. R., Jr., Zachariah, M. R., Tsang, W., and Westmoreland, P. R., *Prog. Energy Combust. Sci.* 21: 453 (1996).
 22. Kee, R. J., Grcar, J. F., Smooke, M. D., and Miller, J. A. (1985). *PREMIX: A Fortran Program for Modeling Steady One-Dimensional Premixed Flames*. Sandia Report SAND85-8240.
 23. Kee, R. J., Rupley, F. M., and Miller, J. A. (1989). *CHEMKIN-II: A Fortran Chemical Kinetic Package for the Analysis of Gas Phase Chemical Kinetics*. Rep. No. SAND89-8009, Sandia National Laboratories, Livermore, CA.
 24. Frenklach, M., Wang, H., Goldenberg, M., Smith, G. P., Golden, D. M., Bowman, C. T., Hanson, R. K., Gardiner, W. C., and Lissianski, V. (1995). *GRI-Mech—An Optimized Detailed Chemical Reaction Mechanism for Methane Combustion*. Gas Research Institute Topical Rep. No. GRI-95/0058.
 25. Vagelopoulos, C. M., Egolfopoulos, F. N., and Law, C. K., *Twenty-Fifth Symposium (International) on Combustion*, The Combustion Institute, 1994, p. 1341.
 26. Westbrook, C. K., *Nineteenth Symposium (International) on Combustion*, The Combustion Institute, 1982, p. 127.
 27. Bui-Pham, M. N., Lutz, A. E., Miller, J. A., Desjardin, M., O'Shaugnessy, D. M., and Zondlak, R. J., *Combust. Sci. Technol.* 109:71–91 (1995).
 28. Law, C. K., and Egolfopoulos, F. N., *Twenty-Third Symposium (International) on Combustion*, The Combustion Institute, 1990, p. 413.
 29. Chung, S. H., Chung, D. H., Fu, C., and Cho, P., *Combust. Flame* 106:515 (1996).
 30. Law, C. K., and Egolfopoulos, F. N., *Twenty-Fourth Symposium (International) on Combustion*, The Combustion Institute, 1992, p. 137.
 31. Hertzberg, M. (1982). *The Theory of Flammability Limits: Radiative Losses and Selective Diffusional Demixing*. Bureau of Mines Report of Investigation, RI-8607.

Received 29 May 1997; revised 12 August 1998; accepted 1 September 1998